Organic LETTERS

Letter

pubs.acs.org/OrgLett

Novel Benzimidazole Derivatives as Electron-Transporting Type Host To Achieve Highly Efficient Sky-Blue Phosphorescent Organic Light-Emitting Diode (PHOLED) Device

Jau-Jiun Huang,[†] Man-kit Leung,*[,†,‡] Tien-Lung Chiu,*[,§] Ya-Ting Chuang,[§] Pi-Tai Chou,*[,†] and Yu-Hsiang Hung[§]

[†]Department of Chemistry and [‡]Institute of Polymer Science and Engineering, National Taiwan University, 1 Roosevelt Road Section 4, Taipei 106, Taiwan, R.O.C.

[§]Department of Photonics Engineering, Yuan Ze University, 135 Yuan-Tung Road, Chung-Li 32003, Taiwan, R.O.C.

Supporting Information

ABSTRACT: The development of benzimidazole substituted biphenyls as electron-transporting hosts for bis[2-(4,6-difluorophenyl)pyridinato-C^2,N](picolinato)iridium-(III) is reported. Under the optimized conditions, the organic light-emitting diode (OLED) achieves the maximum current efficiency of 57.2 cd/A, power efficiency of 50.4 lm/W, and external quantum efficiency 25.7%.

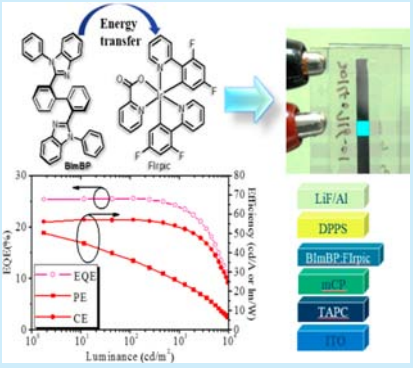

Phosphorescent organic light-emitting diodes (PHOLEDs) have potential in display and lighting applications because of their high theoretical quantum efficiency, which can be, in principle, four times higher than that of the fluorescent based organic light-emitting diodes (OLEDs).[1] To achieve high efficiency, the phosphorescence emitters have to be doped in a host matrix to reduce the probability of triplet−triplet annihilation. Therefore, development of host materials with appropriate optoelectronic properties such as charge carrier mobility, well-matched highest occupied molecular orbital and lowest unoccupied molecular orbital (HOMO−LUMO) levels, optical band gap, morphology, and thermal stability is crucial.[2] With regards to the carrier behavior, the hosts can be at least classified into four categories: (1) hole transporting;[3] (2) bipolar;[4] (3) nonpolar,[5] and (4) electron transporting (ET).[6] Among many high performance blue phosphorescence emitters,[7] bis[2-(4,6-difluorophenyl)pyridinato-C^2,N](picolinato)iridium-(III) (FIrpic) has been shown to exhibit high external quantum efficiency (EQE) over 25%, strongly depending on the host material. Therefore, many hole-transporting and bipolar hosts such as 1,3-(dicarbazol-*N*-yl)benzene (mCP) and derivatives, which achieved current efficiencies (η_c) as high as 60 cd/A, have been successfully developed.[8] In addition, other bipolar hosts have widely been published such as mCPCN, mNBICz, and PPO27.[4a,9] Conversely, examples of highly efficient electron-transporting hosts (ETHs) for FIrpic are rare, except that Lee et al. reported a pyridoindole-based host material named CbBPCb, which is ET dominating and obtained an η_c of 53.6 cd A^{-1} with an EQE of 30%.[10] In our present work, we have explored the possibility of using *N*-phenylbenzimidazole (*N*-PBI) based molecules, including **BImBP** and **o-PhBz** (Scheme 1), as effective ETHs for FIrpic. A high current efficiency of 57.2 cd/A with low efficiency roll-off, a power efficiency (η_p) of 50.4 lm/W, an EQE of 25.7% in the class, and a Commission International de l'Eclairage coordinate (CIE) of (0.15, 0.38) were found. The PHOLED can maintain a high η_c of 53 cd/A at 1000 cd/m^2.

Scheme 1. Chemical Structures of the *N*-PBI Derivatives

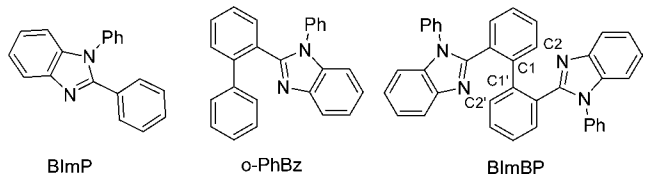

To be an ideal host material in PHOLEDs, the host must have a triplet energy (E_T) higher than that of the doped guest to prevent reverse energy transfer. Moreover, to reduce the hole and electron injection barriers, the HOMO/LUMO level of the host should correspond with the HOMO/LUMO levels of the hole- and ET-transporting layers, respectively. *N*-PBI derivatives have been proven effective for electron injection and transport.

Received: September 5, 2014
Published: October 9, 2014

dx.doi.org/10.1021/ol502602t | *Org. Lett.* 2014, 16, 5398−5401

For example, 1,3,5-tris(*N*-phenylbenzimidazol-2-yl)benzene (TPBi) has been widely used as an ET layer in PHOLEDs. However, to the best of our knowledge, *N*-PBI derivatives have never been used as ETHs for FIrpic-based PHOLEDs. To maintain the high E_T, we adopted a strategy of connecting the *N*-PBI group at the 2,2′-position of biphenyl. We expect that the inter-ring steric hindrance would force the aromatic rings aligned in noncoplanar conformations and thus interrupt the π conjugation. To further understand the electronic interactions between the facing *N*-PBI group, the mono-*N*-PBI-substituted **o-PhBz** has been prepared and studied for comparison.

The syntheses were facile with a high product total yield (greater than 54%), which started from 2-phenylbenzoic acid and 2,2′-biphenyldicarboxylic acid that were converted to the corresponding acyl chloride, followed by reaction with 2-aminodiphenylamine under acid catalyzed dehydrative cyclization conditions to give **o-PhBz** and **BImBP** in multigram scale (Scheme S1 and synthetic procedures).

o-PhBz and **BImBP** have a high decomposition temperature (T_d) of 267 and 350 °C respectively (Figure S5). However, **o-PhBz** and **BImBP** show different morphological behavior. **o-PhBz** presents a low glass-transition temperature (T_g) of 47 °C. In contrast, **BImBP** shows dramatically different phase stability with no T_g being observed below 270 °C; only an endothermic peak associated with the melting point at 275 °C was observed in the heating process while recrystallization was observed at 213 and 220 °C in the cooling process. This behavior indicates that **BImBP** favors a native crystalline form. Nevertheless, to our surprise, the high tendency of crystallization does not hamper the PHOLED performances (vide infra).

X-ray crystallography, a useful tool for understanding material properties,[11] illustrated that molecular stacking of **BImBP** is very different from that of **o-PhBz**. Perhaps due to the steric repulsions between the *N*-PBI substituents and biphenyl moieties, the biphenyl moiety of **BImBP** possesses noncoplanar alignment with a C2 proper rotational axis perpendicular to the biphenyl axis. The C2−C1−C1′−C2′ dihedral angle of 49.9° was found for the biphenyl unit. Similar to **BImBP**, **o-PhBz** has the C2−C1−C1′−C2′ dihedral angle of 45.3°. Both dihedral angles are larger than 45°, indicating orthogonal alignments of the aromatic units. This will strongly affect the electronic properties of the molecules. For example, the lowest triplet state (T_1) therefore is maintained at high energy levels due to disruption of the π-conjugations that is clearly observed in the phosphorescence measurement. Presumably the short face-to-face intrabenzimidazole distance of 3.35 Å allows through-space interactions between the benzimidazole units. Furthermore, the short interbenzimidazole distance of 5.28 Å between the adjacent molecules along the *b* axis of the unit cell also allows effective electron hopping between the **BImBP**s units (Figure 1).

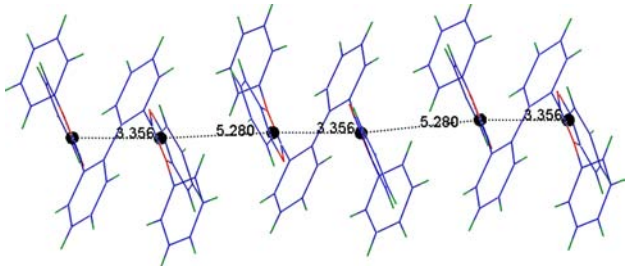

Figure 1. Single crystal molecular packing of **BImBP**s.

o-PhBz and **BImBP** show strong absorption at wavelengths (λ) 270−335 nm that are characteristic for the $\pi-\pi^*$ transitions of the *N*-PBI chromophores (Figure S6). Optical gaps of 3.78 and 3.76 eV (Table 1) were estimated respectively according to their λ_{onset} values. The small spectral difference between **BImP** (λ_{max} of 295 nm), **o-PhBz**, and **BImBP** may be due to the orthogonal conformation of the biphenyl bridge that interrupts the π-conjugation in **BImBP**, causing the *N*-PBI units to function as independent chromophores. On the other hand, the fluorescence emissions, peaking at 385 and 378 nm and spanning the range 350−430 nm, respectively, well overlap with the MLCT absorption of FIrpic; this would allow effective energy transfer from the excited state of **o-PhBz** and **BImBP** to that of FIrpic. The triplet energies 3.08 and 2.89 eV were estimated on the basis of the phosphorescent λ_{onset} respectively. The E_T is high enough to prevent the reverse energy transfer from the FIrpic blue phosphor (E_T of 2.65 eV) to the host in the triplet manifold, and hence in principle both are potentially useful host materials for FIrpic in PHOLEDs.

Table 1. Electrochemical Data and Photophysical Data for BImBPs and the References

host	λ_{abs}^{onset} (nm)[a]	$\lambda_{PH}^{Max/onset}$ (nm)[b]	E_T/E_g (eV)	E_{HOMO}[c]/E_{LUMO}[d] (eV)
BImP	326	479/391	3.17/3.81	−6.22/−2.41 (−2.46)[e]
o-PhBz	328	480/403	3.08/3.78	−6.17/−2.39 (−2.44)[e]
BImBP	330	550/430	2.89/3.76	−6.12/−2.36 (−2.42)[e]
				−6.18/−2.36[f]

[a]Measured in THF (10^{-5} M). [b]Measured in THF (10^{-6} M). [c]Estimated by CV with Bu_4NClO_4 (0.1 M) as supporting electrolyte vs Ag/AgCl. The E_{HOMO} was estimated in CH_2Cl_2 according to the Forrest approach.[12] [d]$E_{LUMO} = E_{HOMO} + E_g$. [e]The E_{LUMO} was estimated by CV in DMF.[13] [f]By AC2 and thin-film optical gap.

The electrochemical properties were evaluated by cyclic voltammetry (CV) and differential-pulse voltammetry (DPV) in DMF and CH_2Cl_2, respectively, using Bu_4NClO_4 (10^{-1} M) as the supporting electrolyte and Ag/AgCl as the reference electrode, and calibrated against ferrocene/ferrocenium (Fc^+/Fc) (Figures S7−S8). In the reduction scans, **o-PhBz** and **BImBP** exhibit irreversible multireduction waves with the first DPV peak potential at −2.56 and −2.59 V (vs Fc^+/Fc) respectively. In the oxidation scans, **o-PhBz** shows a single irreversible oxidation wave with the DPV peak potential at +1.14 V. On the other hand, **BImBP** shows double oxidation waves peaking at +1.10 and 1.38 V. Double-oxidation waves indicated that the *N*-PBI substituents of **BImBP** are electronically coupled in the cationic states; this splits the oxidation wave into two with the first oxidation being slightly stabilized in comparison to that of **BImP** and **o-PhBz**. The CV analysis suggested that the presence of the *N*-PBI functionality is beneficial for either electron or hole injection and transport in the PHOLED.

The HOMO level of thin films of **BImBP** and **o-PhBz** was further measured by AC-2 photoelectron spectrometry (Figure S9). The HOMO level of −6.18 eV for **BImBP** was found accordingly. Perhaps due to having a relatively low density of the benzimidazole units in the matrix, the HOMO level of **o-PhBz** is too deep and the work function cannot be accurately extrapolated from the spectrum. However, the trend of the curve suggests that the HOMO level is ~0.25 eV deeper than that

dx.doi.org/10.1021/ol502602t | *Org. Lett.* 2014, 16, 5398−5401

of **BImBP**. The LUMO levels of −2.36 eV for **BImBP** was estimated according to the equation of $E_{LUMO} = E_{HOMO} + E_g$, where E_g is optical band gap of the thin film. The HOMO/LUMO values are in good agreement with those of **BImBP** and **o-PhBz** obtained from DPV, which were −6.12/−2.36 and −6.17/−2.39 eV respectively. The appropriate HOMO/LUMO alignment not only benefits the hole and electron injection into the layer but also allows **BImBP** to act as an effective host for FIrpic (Figures S10, S13); these findings are very important because the family of *N*-PBI are typically considered as ET materials only.

To gain insight into the electronic properties, the hole and electron mobility of **BImBP** and **o-PhBz** were examined by using the hole- and electron-only devices. In these experiments, the multilayer devices were prepared by thermal vapor deposition methods under high vacuum conditions. The hole-transporting properties were evaluated by a device of ITO/MoO_3(1 nm)/host(100 nm)/MoO_3(1 nm)/Al(100 nm), and the ET properties were examined by a device of glass/Al(50 nm)/LiF(1 nm)/host(100 nm)/LiF(1 nm)/Al(100 nm).

The layer thicknesses of **BImBP** and **o-PhBz** in both types of devices were set to 100 nm for a fair comparison. The plot of current density of single-charge versus applied electrical voltage of **BImBP** in Figure 2a (Figure S11) shows that the electron current density is much higher in general than the hole current density at the device-operation electrical voltage, indicating that electrons are the major carriers in **BImBP**. Under normal operating electrical voltage, the electron current density overwhelms the hole-current density by orders of magnitude. At 10 V, over 4 orders of magnitude discrepancy was recorded. The field independent mobilities of $\mu_0 = 1.8 \times 10^{-5}$ cm^2/(V s) for the electron and $\mu_0 = 6.2 \times 10^{-10}$ cm^2/(V s) for the hole were found respectively (Figure S12). These observations suggest that **BImBP** is an excellent ET material. During the measurement, it is noteworthy that the device of **o-PhBz** is subject to damage at higher applied electrical voltage due perhaps to the lower thermal stability (vide supra); short circuiting of the device was observed when the applied electrical voltage was >10 V. This observation hampers the use of **o-PhBz** as a host for PHOLEDs.

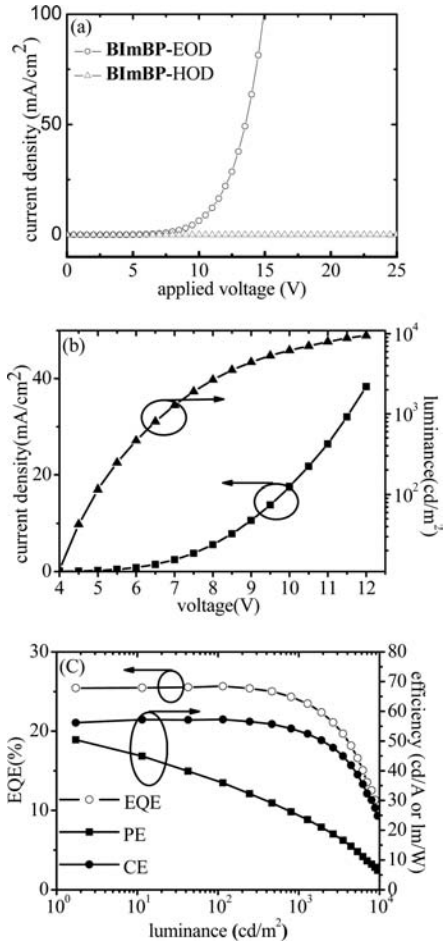

Figure 2. (a) Plot of current density (I) versus applied electrical voltage (V) for hole-only and electron-only device. (b) I−V−Luminance plot and (c) EL efficiency versus brightness plot.

The optimized device configuration is shown as follows: ITO/4,4′-cyclohexylidenebis[*N*,*N*-bis(4-methylphenyl)benzenamine] (TAPC, 45 nm)/mCP (10 nm)/**BImBP**: 12% FIrpic (35 nm)/diphenylbis[4-(pyridin-3-yl)phenyl]silane (DPPS, 55 nm)/LiF (0.9 nm)/Al (120 nm). Other data including the energy level alignment, FIrpic concentration effects, and EL spectral properties are shown in Figures S13−S16. To optimize the recombination efficiency in the emitting layer, the thicknesses of the DPPS and emitting layers were adjusted to enable the hole−electron balance. Since **BImBP** shows superb electron transport properties, TAPC, with high hole mobility and high triplet energy (μ_h of 1.0×10^{-2} cm^2/(V s), E_T of 2.87 eV),[14] was employed as the hole-transporting layer. In addition, the presence of the layer of *m*CP was found to be essential to maintain the high efficiency. Figure 2b−2c show the current density−voltage−luminance curves of the blue PHOLEDs, with the luminance up to 9513 cd/m^2 at 38.3 mA/cm^2, maximum η_p up to 50.4 lm/W, maximum η_c up to 57.2 cd/A, and maximum EQE up to 25.7%.

Despite **BImBP** being an ETH, we believe FIrpic dopant also acts as an electron trap, which balances the hole and electron in the emitting layer to increase the recombination efficiency. In addition, using TAPC as the hole transport layer that has a high E_T helps confine the charge and exciton inside the emitting layer and hence enhances the performance of the **BImBP** device.[10,15] The blue PHOLED of **BImBP** exhibits maximum emission peaking at 472 nm which is typical for the FIrpic emission, and its CIE coordinate is (0.15, 0.38) at 4 V (Figure S17). No emission from the host or the charge transport materials was observed, indicating complete energy transfer from **BImBP** to FIrpic and full charge confinement inside the emitting layer. This is further supported by the fluorescence lifetime study, using a time-correlated single photon counting technique. Instead of having a long fluorescence lifetime τ of 3.57 ns in pure **BImBP** film, the lifetime is significantly shortened (τ < 50 ps) by doping with FIrpic (6%), indicating the effectiveness of the energy transfer process (Figure S10).

In summary, we report herein the design of **BImBP** as well as its synthesis, characterization, and application in an OLED. First, the high production yield is important for scalable synthesis and future application. Furthermore, the intramolecular electronic interactions between the N-PBI units significantly reduce the oxidation potential, leading to the HOMO level of −6.18 eV. This permits effective hole injection into **BImBP** for exciton recombination and light emission. In addition, the X-ray crystallographic analysis illustrates that the packing of the molecules allows effective electron hopping inside the matrix. By employing **BImBP** as the host matrix for FIrpic, we obtained a high current efficiency of 57.2 cd/A based on the ET host, with

dx.doi.org/10.1021/ol502602t | *Org. Lett.* 2014, 16, 5398−5401

an EQE of 25.7%. The device performance of **BImBP** is comparable to that of previously reported high-performing devices with hole-transporting or bipolar hosts.

■ ASSOCIATED CONTENT

Supporting Information

NMR data; UV−vis, FL, and phosphorescence spectra; CV, TGA and DSC, CIF data; and device performance. This material is available free of charge via the Internet at http://pubs.acs.org.

■ AUTHOR INFORMATION

Corresponding Authors

* E-mail: mkleung@ntu.edu.tw (M.-k.L.).
*E-mail: tlchiu@saturn.yzu.edu.tw (T.-L.C.).
*E-mail: chop@ntu.edu.tw (P.-T.C.).

Notes

The authors declare no competing financial interest.

■ ACKNOWLEDGMENTS

This work was supported by the Ministry of Science and Technology (MOST), R.O.C., under Grant MOST 101-2113-M-002-010-MY3, 103-3113-E-155-001, 102-2221-E-155-047, and 102-2622-E-155-008-CC3, and Bureau of Energy, Ministry of Economic Affairs, R.O.C. under Grant No. 102-E0616. We also thank Prof. Jiun-Haw Lee, Department of Electrical Engineering, National Taiwan University, for his invaluable opinion and suggestions and Prof. Yu-Tai Tao, Institute of Chemistry, Academia Sinica, for AC-2 measurement.

■ REFERENCES

(1) (a) Tang, C. W.; VanSlyke, S. A. *Appl. Phys. Lett.* **1987**, *51*, 913−915. (b) Baldo, M. A.; O'Brien, D. F.; You, Y.; Shoustikov, A.; Sibley, S.; Thompson, M. E.; Forrest, S. R. *Nature* **1998**, *395* (6698), 151. (c) Adachi, C.; Baldo, M. A.; Thompson, M. E.; Forrest, S. R. *J. Appl. Phys.* **2001**, *90*, 5048−5051. (d) Xiao, L.; Chen, Z.; Qu, B.; Luo, J.; Kong, S.; Gong, Q.; Kido, J. *Adv. Mater.* **2011**, *23*, 926−952.

(2) (a) Chaskar, A.; Chen, H.-F.; Wong, K.-T. *Adv. Mater.* **2011**, *23*, 3876−3895. (b) Tao, Y.; Yang, C.; Qin, J. *Chem. Soc. Rev.* **2011**, *40*, 2943−2970.

(3) (a) Gong, S.; He, X.; Chen, Y.; Jiang, Z.; Zhong, C.; Ma, D.; Qin, J.; Yang, C. *J. Mater. Chem.* **2012**, *22*, 2894−2899. (b) Holmes, R. J.; Forrest, S. R.; Tung, Y.-J.; Kwong, R. C.; Brown, J. J.; Garon, S.; Thompson, M. E. *Appl. Phys. Lett.* **2003**, *82*, 2422−2424.

(4) (a) Lin, M.-S.; Yang, S.-J.; Chang, H.-W.; Huang, Y.-H.; Tsai, Y.-T.; Wu, C.-C.; Chou, S.-H.; Mondal, E.; Wong, K.-T. *J. Mater. Chem.* **2012**, *22*, 16114−16120. (b) Leung, M.-k.; Hsieh, Y.-H.; Kuo, T.-Y.; Chou, P.-T.; Lee, J.-H.; Chiu, T.-L.; Chen, H.-J. *Org. Lett.* **2013**, *15*, 4694−4697. (c) Cho, Y.-J.; Yook, K.-S.; Lee, J.-Y. *Adv. Mater.* **2014**, *26*, 4050−4055. (d) Lee, C. W.; Lee, J. Y. *Dyes Pig.* **2014**, *109*, 1−5.

(5) Ren, X.; Li, J.; Holmes, R. J.; Djurovich, P. I.; Forrest, S. R.; Thompson, M. E. *Chem. Mater.* **2004**, *16*, 4743−4747.

(6) (a) Leung, M.-k.; Yang, C.-C.; Lee, J.-H.; Tsai, H.-H.; Lin, C.-F.; Huang, C.-Y.; Su, Y. O.; Chiu, C.-F. *Org. Lett.* **2006**, *9*, 235−238. (b) Chen, H.-F.; Yang, S.-J.; Tsai, Z.-H.; Hung, W.-Y.; Wang, T.-C.; Wong, K.-T. *J. Mater. Chem.* **2009**, *19*, 8112−8118. (c) Jeon, S. O.; Lee, J. Y. *Org. Electron.* **2011**, *12*, 1893−1898. (d) Fukagawa, H.; Yokoyama, N.; Irisa, S.; Tokito, S. *Adv. Mater.* **2010**, *22*, 4775−4778.

(7) (a) Sasabe, H.; Takamatsu, J.-i.; Motoyama, T.; Watanabe, S.; Wagenblast, G.; Langer, N.; Molt, O.; Fuchs, E.; Lennartz, C.; Kido, J. *Adv. Mater.* **2010**, *22*, 5003−5007. (b) Udagawa, K.; Sasabe, H.; Cai, C.; Kido, J. *Adv. Mater.* **2014**, *26*, 5062−5066.

(8) Chopra, N.; Lee, J.; Zheng, Y.; Eom, S.-H.; Xue, J.; So, F. *ACS Appl. Mater. Interfaces* **2009**, *1*, 1169−1172.

(9) (a) Pan, B.; Wang, B.; Wang, Y.; Xu, P.; Wang, L.; Chen, J.; Ma, D. *J. Mater. Chem. C* **2014**, *2*, 2466−2469. (b) Son, H. S.; Seo, C. W.; Lee, J. Y. *J. Mater. Chem.* **2011**, *21*, 5638−5644.

(10) Lee, C. W.; Lee, J. Y. *Adv. Mater.* **2013**, *25*, 5450−5454.

(11) Xu, X.; Yang, X.; Dang, J.; Zhou, G.; Wu, Y.; Li, H.; Wong, W.-Y. *Chem. Commun.* **2014**, *50*, 2473−2476.

(12) Andrade, B. W. D.; Datta, S.; Forrest, S. R.; Djurovich, P.; Polikarpov, E.; Thompson, M. E. *Org. Electron.* **2005**, *6*, 11−20.

(13) Djurovich, P. I.; Mayo, E. I.; Forrest, S. R.; Thompson, M. E. *Org. Electron.* **2009**, *10*, 515−520.

(14) Lee, J.; Chopra, N.; Eom, S.-H.; Zheng, Y.; Xue, J.; So, F.; Shi, J. *Appl. Phys. Lett.* **2008**, *93*, 123306(1−3).

(15) Fan, C.; Zhu, L.; Liu, T.; Jiang, B.; Ma, D.; Qin, J.; Yang, C. *Angew. Chem., Int. Ed.* **2014**, *53*, 2147−2151.